applied sciences

MDPI

Article

A CFD Results-Based Approach to Investigating Acoustic Attenuation Performance and Pressure Loss of Car Perforated Tube Silencers

Hao Zhang, Wei Fan and Li-Xin Guo *

School of Mechanical Engineering and Automation, Northeastern University, Shenyang 110819, China; peterat2011@foxmail.com (H.Z.); 1410110@stu.neu.edu.cn (W.F.)
* Correspondence: lxguo@mail.neu.edu.cn

Received: 1 March 2018; Accepted: 29 March 2018; Published: 2 April 2018

Abstract: This paper proposes an approach to investigating the effect of different temperatures and flow velocities on the acoustic performance of silencers in a more accurate and meticulous fashion, based on steady computational results of the flow field inside the silencer using computational fluid dynamics (CFD). This approach can transfer the CFD results—including temperature and flow velocity distribution—to acoustic meshes by mesh mapping. A numerical simulation on the sound field inside the silencer is then performed, using the CFD results as a boundary condition. This approach facilitates the analysis of complex silencer designs such as perforated tube silencers, and the numerical predictions are verified by a comparison with available experimental data. In the case of the three-pass perforated tube silencer of a car, the proposed approach is implemented to calculate the transmission loss (*TL*) of the silencer at different temperatures and flow velocities. We found that increasing the air temperature shifts the TL curve to a higher frequency and reduces the acoustic attenuation at most frequencies. As the air flow increases, the curve moves to a slightly lower frequency and the acoustic attenuation increases slightly. Additionally, the pressure loss of perforated tube silencers could be calculated according to the total pressure distribution of their inlet and outlet from the steady computational results using CFD.

Keywords: perforate tube silencer; transmission loss (*TL*); pressure loss; computational fluid dynamics (CFD); temperature; air flow velocity

1. Introduction

The silencer is the main device used for suppressing automobile noise. The most important goal for a high-performance silencer is to simultaneously have good aerodynamic and acoustic attenuation characteristics. However, these often contradict each other. Perforated tube silencers are well-balanced in terms of both characteristics. Thus, they are applied extensively to the exhaust systems of automobiles.

Pressure loss is the main indicator used for evaluating the aerodynamic performance of a silencer. It has a negative influence on the efficiency of an engine. If the loss exceeds the backpressure limit, it will result in reduced engine power and an increase in fuel consumption [1]. Currently, the pressure loss is predicted by performing a 3D steady computation using computational fluid dynamics (CFD). This method has been widely accepted among researchers because of its high level of accuracy and adaptability [2–4]. Middelberg et al. [5] computed the pressure loss of a simple expansion chamber muffler using a CFD simulation. Lee et al. [6] predicted the pressure loss of concentric tube silencers with five different patterns of perforated elements using CFD analysis. Ren et al. [7] employed the

CFD approach to predict the pressure loss of an exhaust muffler, which was influenced by the insert duct, the position of the baffle, and the inlet air velocity.

Transmission loss (*TL*) is one of the most important indicators used for evaluating the acoustic attenuation performance of a silencer. The gas from an automotive engine has a high temperature and speed, which will have a strong influence on the acoustic attenuation performance. High temperature changes, gas density, sound velocity and acoustic impedance [8], and the effects of flow velocity embody two sides: one is to affect the sound wave propagation in a medium, and the other is to reduce aerodynamic noise resulting from turbulence [9]. Various theoretical and experimental studies were conducted in the past in order to investigate the acoustic attenuation performance of a silencer under the influence of different temperatures and air flow [10–12]. Kim et al. [13] investigated the acoustic characteristics of an expansion chamber with a constant mass flow and a steady temperature gradient. Tsuji et al. [14] applied finite element and boundary element methods to evaluate the acoustic wave transmission characteristics in a medium with uniform and steady mean flow. Kirby [15] compared two numerical methods and two analytical methods of modelling automotive dissipative silencers with a uniform mean gas flow of Mach number (M). The comparison indicated a close similarity to the *TL* predictions that were obtained for the silencers that were examined. With the rapid development of high-performance computers, the 3D numerical simulation method plays an increasingly significant role in sound field analysis. Broatch et al. [16] proposed a 3D time-domain technique based on the CFD approach to calculate the *TL* of exhaust mufflers with different chambers. Sánchez-Orgaz et al. [17] proposed a hybrid finite element approach—combining an acoustic velocity potential formulation in the central airway with a pressure-based wave equation in the outer chamber—to study the *TL* of perforated dissipative silencers with heterogeneous properties in the presence of mean flow. Dong et al. [18] employed the CFD approach to perform a 3D steady computation and obtain a temperature distribution inside a two-pass perforated tube silencer, and then defined the elements with a 5 °C difference in temperature as a collection. The air parameters of the corresponding temperatures were assigned to the defined collections using SYSNOISE software, in order to calculate the *TL*.

However, most of the present works associated with predicting the *TL* of perforated tube silencers assume the mean flow to be uniform. Similarly, the temperature fields are simplified as constant or linear fields, which may result in inaccurate analytical results—especially in the case of silencers with complicated temperature and flow velocity distributions. In light of the aforementioned disadvantages, this paper proposes an approach based on CFD results to investigate the acoustic attenuation performance of silencers. This approach comprises the following steps: (1) the flow field inside the silencer is calculated by performing a 3D steady computation using CFD; (2) the CFD results—including temperature and air flow velocity—are transferred to acoustic meshes by mesh mapping, so that the results can be used as a boundary condition of sound field analysis; (3) the *TL* of the silencer is calculated at a high temperature and air flow. Compared to previous works, the proposed approach avoids the use of simplified temperature and flow velocity distributions. Consequently, the effects of temperature variation and air flow on the acoustic attenuation performance of silencers can be calculated and observed in greater detail.

This paper proceeds as follows: Following the introduction, Section 2 describes the proposed computational approach and verifies its accuracy. Section 3 builds an internal fluid model of a perforated tube silencer of a car, and generates CFD meshes and acoustic meshes of the model, respectively. Following this, a 3D steady computation using CFD is performed in order to calculate the pressure loss of the silencer and obtain its temperature and flow velocity distributions. Section 4 employs the proposed approach to investigate the acoustic attenuation performance of the silencer under the influence of different temperatures and air flow. Section 5 concludes the study.

2. Methods

2.1. Mesh Mapping

The most critical step in the proposed approach to calculating the acoustic attenuation of silencers is to set a mesh mapping for transferring data. The mesh mapping is used to transfer the node data of the CFD mesh (source mesh) into the acoustic mesh (target mesh). However, there is not usually a one-to-one correspondence between the nodes of different meshes. Thus, an appropriate mapping algorithm should be employed.

A maximum distance algorithm is often applied in Virtual.lab acoustics software to set a mesh mapping between different meshes with the same geometrical shape, but a different density of nodes. The algorithm includes the following two necessary parameters [19]:

1. Number of nodes (N): The maximum number of nodes from the source mesh that are considered for mapping with one node of the target mesh.
2. Maximum distance (R): Only the nodes of the source mesh that lie inside a sphere with a radius R—centered at the node of the target mesh—are taken into account.

The N closest nodes to a given source node are used to transfer data to the target node. The data value assigned to the target node is a weighted average of the values at the N source nodes. The weights are:

$$W_i = \frac{1}{d_i} \Big/ \sum_{i=1}^{N} \frac{1}{d_i}. \tag{1}$$

The transferred value of the target node is then:

$$P_{\text{Target}} = \sum_{i=1}^{N} \frac{P_i^{\text{Source}}}{d_i} \Big/ \sum_{i=1}^{N} \frac{1}{d_i}, \tag{2}$$

where d_i is the distance between the source node and the target node, and P_i^{Source} is the value of the source node.

For example, when the target node is defined as a center, there are three source nodes (N = 3) lying inside a sphere with R = 100 mm. Thus, the mapping data transfer relation is depicted in Figure 1. The value at A is given by:

$$P_{\text{Target}} = \frac{\frac{1}{d_1} P_1^{\text{Source}} + \frac{1}{d_2} P_2^{\text{Source}} + \frac{1}{d_3} P_3^{\text{Source}}}{\frac{1}{d_1} + \frac{1}{d_2} + \frac{1}{d_3}}. \tag{3}$$

After transferring data by the mesh mapping method, Virtual.lab software is used to conduct a numerical simulation on the internal sound field of the silencer, and the TL is then determined by

$$TL = 10 \log_{10} \left(\frac{W_1}{W_2} \right), \tag{4}$$

with

$$W_1 = |p_1|^2 A_1 / Z_1, W_2 = |p_2|^2 A_2 / Z_2. \tag{5}$$

Substituting (5) into (4) yields

$$TL = 10 \log_{10} \left(\frac{p_1 \overline{p_1} Z_2}{p_2 \overline{p_2} Z_1} \frac{A_1}{A_2} \right), \tag{6}$$

where W_1 and W_2 are the acoustic power of the inlet and outlet of the silencer, respectively; p_1 and p_2 are the sound pressure of the incident and the transmitted waves, respectively; $\overline{p_1}$ and $\overline{p_2}$ are conjugate complex numbers of p_1 and p_2, respectively; Z_1 and Z_2 are the acoustic impedance of the inlet and outlet of the silencer, respectively; and A_1 and A_2 are the cross-sectional areas of the inlet and outlet of the silencer, respectively.

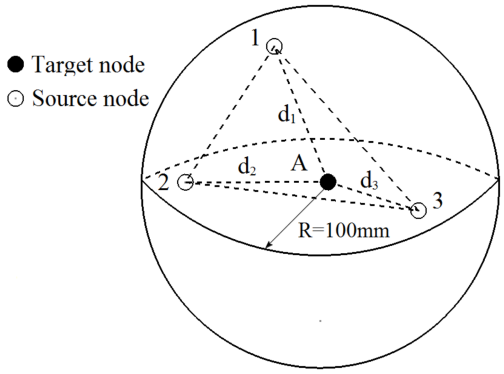

Figure 1. Sketch of data transfer (Number of nodes N = 3, Maximum distance R = 100 mm).

2.2. Method Validation

In order to verify the accuracy of the proposed approach, a straight-through perforated tube silencer with two different perforated patterns that was proposed by the authors of [20,21] and a cross-flow perforated tube silencer that was proposed by the authors of [10] was considered. Previously, Liu et al. [22] employed the 3D time-domain CFD approach to calculate the *TL* of two perforated tube silencers at different flow velocities and temperatures, and their predictions were verified by experimental data. Moreover, they found that the distribution of flow velocity inside the silencer was anisotropic and nonhomogeneous. Therefore, it is not sufficiently accurate to consider the actual gas flow as the mean flow. The approach proposed in this paper avoids this problem effectively.

Figure 2 presents the straight-through perforated tube silencer. The diameters of the inner and outer cavities are d = 32 mm and D = 110 mm, respectively; the length of the silencer is l = 200 mm; the thickness of the wall is 2 mm; and the diameter of the hole and the porosityare dh = 4 mm and σ = 4.7%, respectively, for Pattern 1, and dh = 8 mm and σ = 14.7%, respectively, for Pattern 2. The cross-flow perforated silencer is illustrated in Figure 3. The diameters of the inner and outer cavities are d = 49.3 mm and D = 101.6 mm, respectively; the lengths of tubes on both sides of the baffle are $l_1 = l_2$ = 128.6 mm; each tube is perforated with 160 orifices, with a porosity of 3.9%, a diameter of 2.49 mm; and a wall thickness of 0.81 mm.

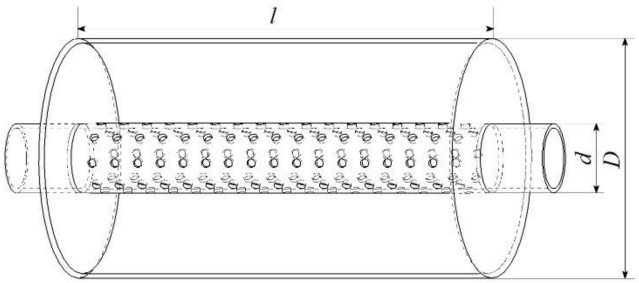

Figure 2. Straight-through perforated tube silencer.

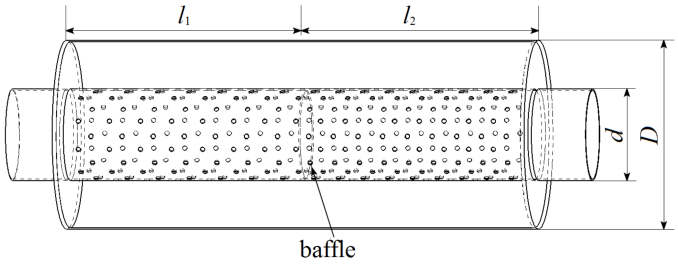

Figure 3. Cross-flow perforated tube silencer.

The proposed approach is applied to calculate the *TL* for the silencers under different boundary conditions, and the predictions were compared with the available measurement results. Figure 4a and 4b compare the *TL* curves of the straight-through perforated tube silencer for Pattern 1 and Pattern 2, respectively. Considering the predictions and measurements at an air flow of $M = 0.1$ and a temperature of $T = 288$ K, it is evident that the predictions are in line with the experimental data. The predicted and measured TL curves for Pattern 1, with $M = 0.2$ and $T = 288$ K, are presented in Figure 5, and it is evident that these predictions are also in line with the experimental data. Figure 6 presents a comparison of the numerical results and the measurements for the cross-flow silencer with an air flow velocity of $v = 17$ m/s and $T = 347$ K, which again presents an excellent agreement.

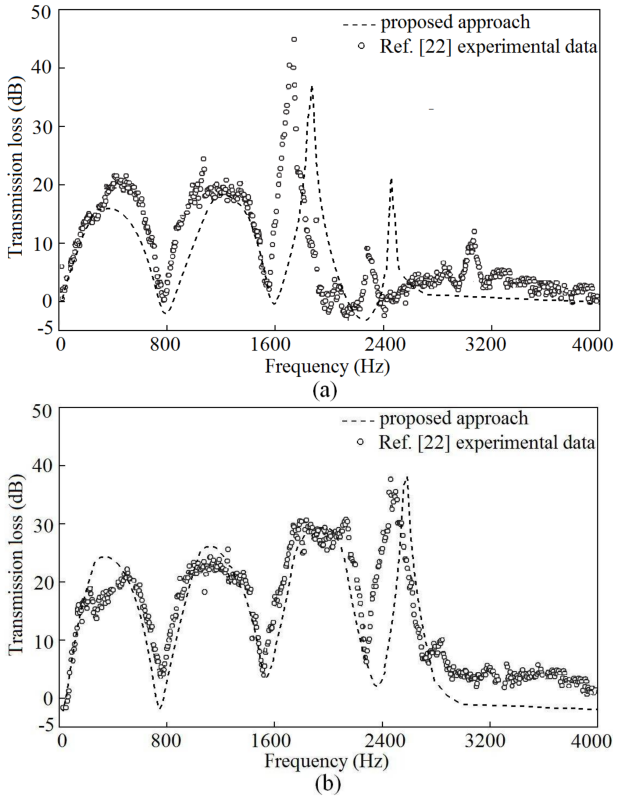

Figure 4. Comparison of the predicted and measured transmission loss (*TL*) for the straight-through perforated tube silencer (Mach number $M = 0.1$, Temperature $T = 288$ K): (**a**) Pattern 1; (**b**) Pattern 2.

Based on the above comparisons, it is evident that the proposed approach displayed a high degree of accuracy in investigating the acoustic attenuation performance of perforated tube silencers. This high degree of accuracy should be attributed to the avoidance of using simplified temperature fields and air flow in the calculation process. In doing so, the actual working condition of the silencer can be

better reflected. Additionally, it must be stated that the computations may be highly time-consuming because there are too many orifices in the silencers, which increases the amount of mesh.

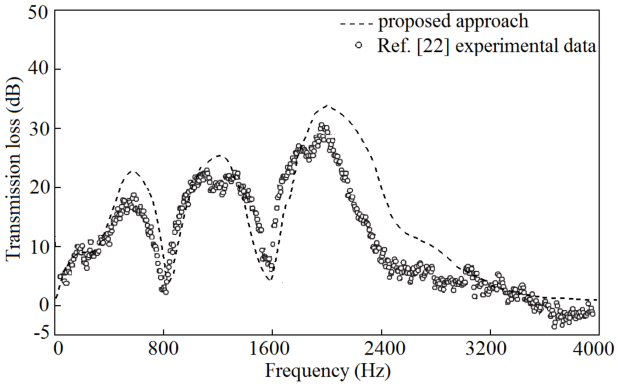

Figure 5. Comparison of the predicted and measured *TL* for Pattern 1 (M = 0.2, T = 288 K).

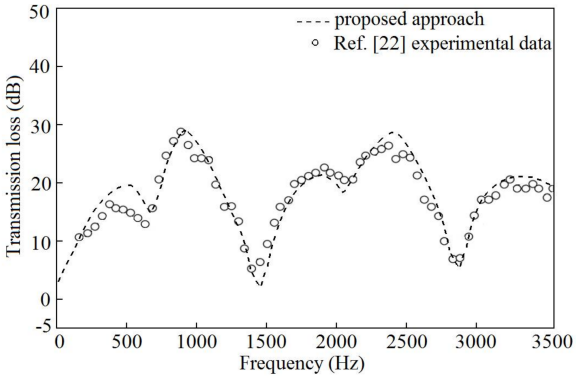

Figure 6. Comparison of the calculated and measured *TL* for the cross-flow silencer (v = 17 m/s, T = 374 K).

3. Modeling and Steady Computation Using CFD

3.1. Modeling

The three-pass perforated tube silencer of a car that is considered in this paper is presented in Figure 7. The silencer is divided into three chambers by two baffles. The inlet tube and the middle buffer tube are respectively perforated by 40 and 48 orifices with 4 mm diameter, and the porosity of the tubes are 2.7% and 5.8%, respectively. There is no perforation in the outlet tube. Additionally, the axes of the three tubes are not on the same plane. Consequently, it is difficult to build a fluid model directly inside the silencer because of its complicated structure. Therefore, firstly CATIA (version V5R20, Dassault Systemes, Paris, France, 2010) software was used to build its structural model, and then it was filled using ANSYS Workbench (version 14.5, ANSYS Inc., Canonsburg, PA, USA, 2012) software to obtain the fluid model. Following this, the fluid model was split into several parts to generate mesh individually. Tetrahedral mesh was applied to the perforation area and the transition tube, and hexahedral mesh was applied to the remaining parts.

Figure 8a,b illustrate the CFD mesh model and the acoustic mesh model of the fluid model, which will be used for CFD steady computation and acoustic computation, respectively. There is a different node density between the two models. The CFD mesh is refined in the perforation area in order to obtain more accurate results. However, the accuracy of the acoustic computation is determined by the overall mesh. Local mesh refinement can not improve its accuracy, and thus the size of the acoustic mesh element should be kept as uniform as possible.

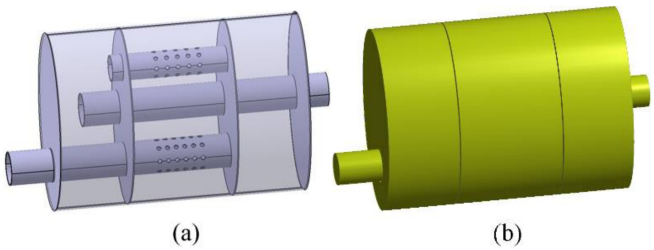

Figure 7. 3D geometrical model for the three-pass perforated tube silencer: (**a**) structural model; (**b**) flow field model.

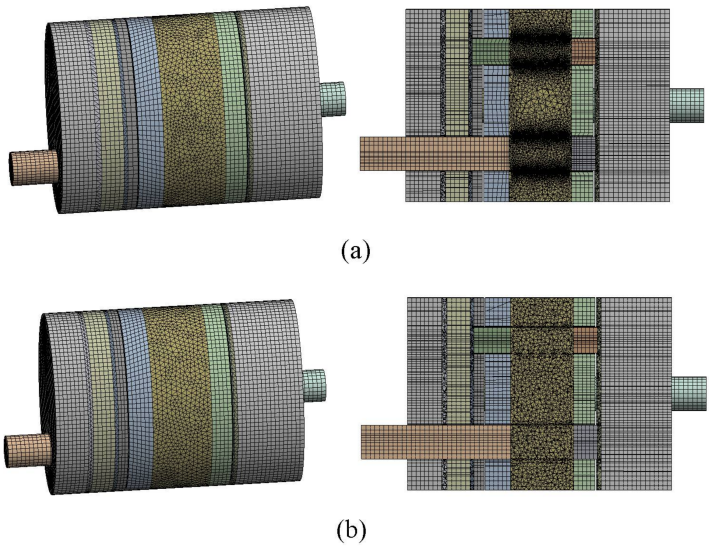

Figure 8. Mesh model for the three-pass perforated tube silencer: (**a**) computational fluid dynamics (CFD) mesh model; (**b**) acoustic mesh model.

The steady flow computation is carried out using the CFD mesh model. The governing equations for pressure velocity coupling—based on a finite volume method—are solved by the Semi-Implicit Method for Pressure Linked Equations (SIMPLE) algorithm. Turbulence is examined using the standard k-epsilon model [23]. The fluid material is air—with the density conforming to the ideal gas law—and is considered as incompressible. The boundary conditions are concretely set as follows: (1) the velocity inlet boundary condition is defined at the inlet of the silencer. According to the information provided by the manufacturer, when the engine runs at 5500 r/min, the velocity and temperature of the inlet are 55 m/s and 760 K, respectively; (2) the pressure outlet boundary condition is defined at the outlet of the silencer, and the gauge pressure is 0 Pa—which is relative to one standard atmospheric pressure; and, (3) the walls are assumed to be stationary—with no slip condition—and adiabatic.

3.2. The CFD Results

Figure 9 shows the temperature distribution in the axial cross sections of the three tubes of the silencer. Overall, the temperature value decreases along the direction of the air flow. There is little difference in temperature between the first and second chambers, where the value is approximately 574 K. However, in the third chamber, the value increases to approximately 670 K. The highest temperature—which is approximately 751 K—occurs in the inlet tube. The temperature in the outlet tube is close to the value of the first chamber, and it is distributed evenly. A greater temperature gradient exists in the perforation area. Additionally, the temperature of the edge chamber is the lowest, which results from the large difference in temperature between the inner and outer walls.

Figure 10 depicts the velocity distribution in the axial cross sections of the three tubes of the silencer. When air flows through the perforation area of the inlet tube and the middle buffer tube, some of the air will enter into the second chamber through the orifices. At this moment, an eddy forms in the perforation area (as shown in Figure 11) because of the disturbance of the airflows with different velocities and flow directions, which may induce a greater velocity gradient in the perforation area. Additionally, there exists a greater velocity gradient next to the nozzle of each tube, resulting from the sudden change of the flow sections.

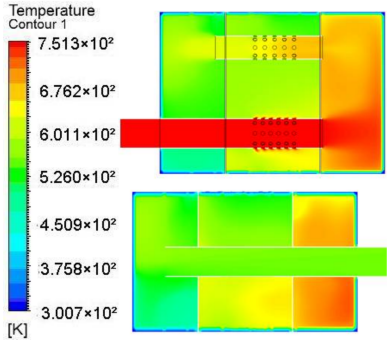

Figure 9. Contour of temperature in the cross section of the silencer.

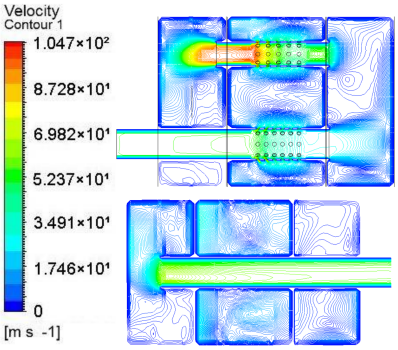

Figure 10. Contour of velocity in the cross section of the silencer.

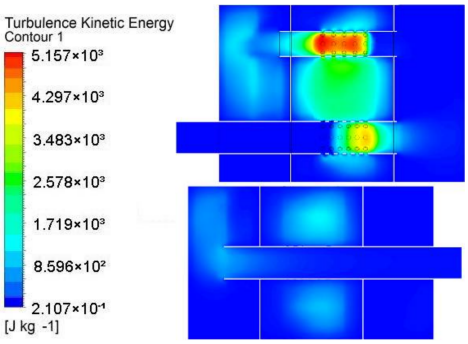

Figure 11. Contour of turbulence kinetic energy in the cross section of the silencer.

Figure 12 illustrates the total pressure distribution in the axial cross sections of the three tubes of the silencer. The highest pressure occurs in the inlet tube—especially in the perforation area—where the value is approximately 23,660 Pa. In the second and third chambers, the pressure is reduced to approximately 19,560 Pa. The middle buffer tube plays the role of the transition region with a greater pressure gradient. Gradually, however, the pressure distribution tends to be uniform in the

first chamber. The pressure is distributed more evenly in the outlet tube than in the other regions, and the value is approximately −2313 Pa (the pressure, which is lower than the atmospheric pressure, may be a result of the Venturi effect).

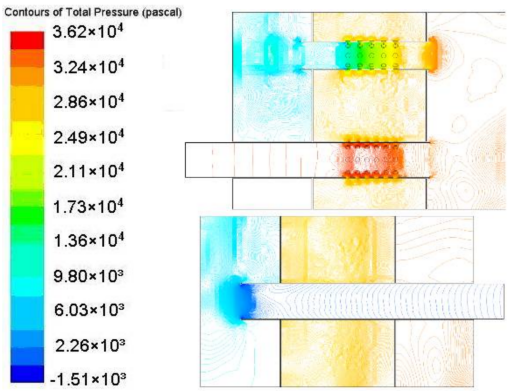

Figure 12. Contour of total pressure in the cross section of the silencer.

Based on the CFD results, it is evident that the distributions of temperature and flow velocity are non-uniform. Therefore, it is not accurate enough to consider them as uniform distributions.

3.3. Pressure Loss Calculation

The pressure loss equals the total pressure difference between the inlet and the outlet of a silencer. Following the method of calculating the pressure loss that was proposed by the authors of [24]—whose accuracy has been validated by experiments—nine evenly distributed points were selected in the cross sections of the inlet and the outlet, respectively. The average total pressure of the nine points was considered to be the total pressure of the corresponding cross section. Therefore, the pressure loss could be expressed as

$$\Delta p = \overline{p_{t_1}} - \overline{p_{t_2}}, \tag{7}$$

where $\overline{p_{t_1}}$ is the total pressure of the inlet, and $\overline{p_{t_2}}$ is the total pressure of the outlet.

Figure 13 presents the cross section of the silencer in question for the pressure loss calculation. The total pressure distribution—predicted by the steady computation using CFD—is applied to obtain the pressure loss of the silencer. The value of the pressure loss is approximately 37,710 Pa. The following explanation is a plausible explanation for the pressure loss that occurred: When air flow moves from the chamber to the tube—or vice versa—the mechanical energy of the air flow is reduced dramatically because of the sudden change of the flow sections. Moreover, there are large-scale eddy zones present in the perforation area that restrict air flow and lead to energy dissipation, which results from the increased turbulence kinetic energy (as shown in Figure 11).

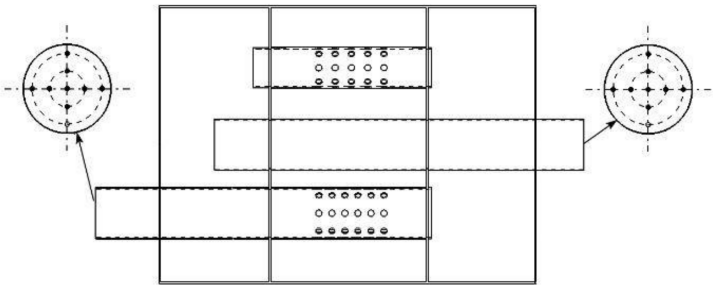

Figure 13. The selected points for the total pressure calculation in the cross sections of the inlet and outlet of the silencer.

4. Sound Field

4.1. Check the Maximum Frequency Value of the Acoustic Mesh

When there is mean flow, the maximum frequency value that is allowed by the acoustic mesh is defined by

$$f_{\max} = \frac{c(1-M)}{6L}, \tag{8}$$

where c is the local sound velocity, M is the mean flow Mach number, and L is the mesh element size [19]. Therefore, the calculated frequency must satisfy the condition $f \leq f_{\max}$ in order to guarantee accuracy during the acoustic calculation. This means that the maximum size of the acoustic mesh should be small enough to allow at least six elements to fit into the wavelength of the calculated frequency.

The CFD results that were acquired in Section 3.2—including the temperature and flow velocity—are transferred to the acoustic mesh (presented in Figure 8b) by mesh mapping. Following the data transfer, the maximum frequency value of the investigated acoustic mesh was obtained through checking the maximum frequency report in Virtual.Lab. The observed value is 3676.1 Hz. The noise frequency that needs to be calculated for the silencer is usually below 3000 Hz. Therefore, the investigated acoustic mesh could guarantee computational accuracy.

4.2. Effects of Temperature Changes on the TL of the Silencer

Prior to performing the acoustic computation, the inlet of the silencer is supplied with a unit vibration velocity source. Additionally, an anechoic end duct property is defined at the end of the outlet to simulate the anechoic termination condition. It is known that the existing acoustic mesh is valid up to a frequency of 3676.1 Hz. Therefore, the analysis is conducted from 20 Hz to 2000 Hz, in linear steps of 10 Hz. Additionally, an input point and an output point are chosen from the inlet and the outlet of the silencer, respectively. Figure 14 presents the sound pressure level of the inlet and outlet of the silencer, calculated by the proposed approach. Figure 14a–c present the sound pressure level of the inlet and outlet of the silencer with the same flow velocity but different temperatures.

Based on the sound pressure of the inlet and the outlet, the *TL* of the silencer is calculated using Equation (6). Figure 15 indicates the *TL* predictions with the same flow velocity (55 m/s) and different temperatures. It may be noted that, as the temperature rises, the *TL* curves move to a higher frequency and the acoustic attenuation is reduced at most frequencies. Considering the *TL* curves from Figure 15a as an example, a valley at 850 Hz is moved to 1160 Hz with an increase in temperature from 560 K to 760 K. Similarly, a peak moves from 1240 Hz to 1560 Hz, while their corresponding TL values are reduced by 10 dB and 20 dB, respectively.

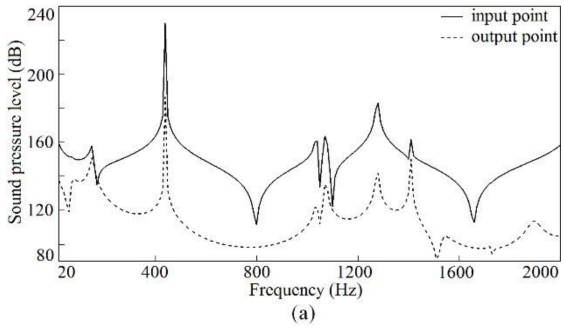

Figure 14. *Cont.*

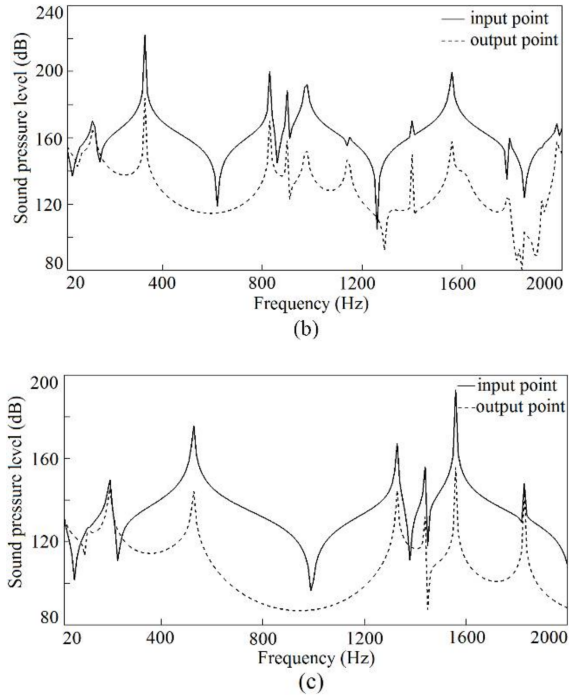

Figure 14. The sound pressure level of the inlet and outlet of the silencer (v = 55 m/s): (**a**) T = 760 K; (**b**) T = 560 K; (**c**) T = 960 K.

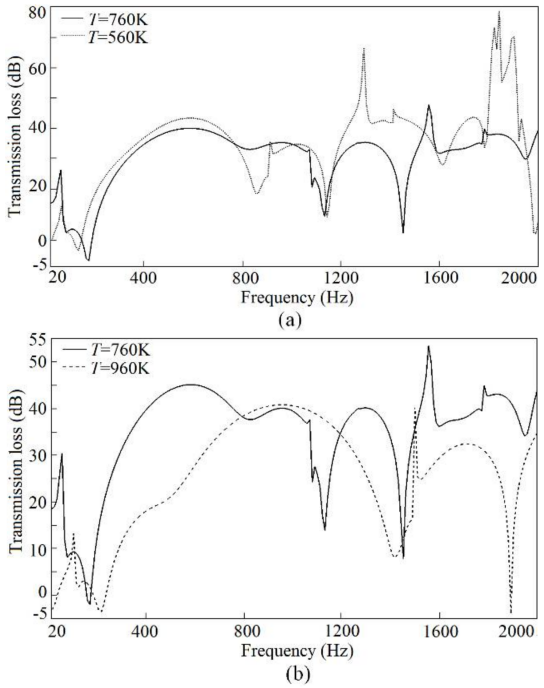

Figure 15. Effects of temperature on the TL of the silencer (v = 55 m/s) : (**a**) 760 K versus 560 K; (**b**) 760 K versus 960 K.

4.3. Effects of Flow Velocity Changes on the TL of the Silencer

It is evident from the flow velocity distribution in Figure 10 that the velocity inside the silencer is lower. Therefore, it is assumed that the air flow mainly influences the sound wave propagation, and the

turbulence noise is neglected [25]. Following the proposed approach, the sound pressure level curves of the inlet and outlet of the silencer—with the same temperature but different flow velocities—are presented in Figure 16.

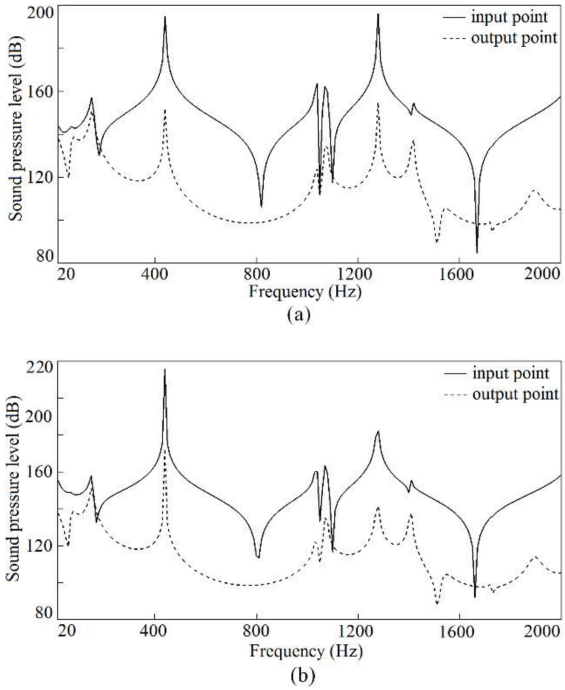

Figure 16. The sound pressure level of the inlet and outlet of the silencer (T = 760 K): (**a**) v = 20 m/s; (**b**) v = 35 m/s.

Figure 17 indicates the effects of increasing the flow velocity on the *TL* predictions at the same temperature (760 K). It can be observed that, as the velocity goes up, the *TL* curves move to a slightly lower frequency and the acoustic attenuation is increased slightly at most frequencies. The variation of the TL curve may be attributed to the fact that the higher velocity increases the acoustic resistance of the perforations and reduces the effective flow area of the orifices [26]. This causes the frequency response of the silencer to differ from a static state. Generally, however, the propagation of the sound wave is only changed dramatically if the air flow Mach number is greater than 0.3 [27]. Therefore, the variation of the curves in Figure 17 is small.

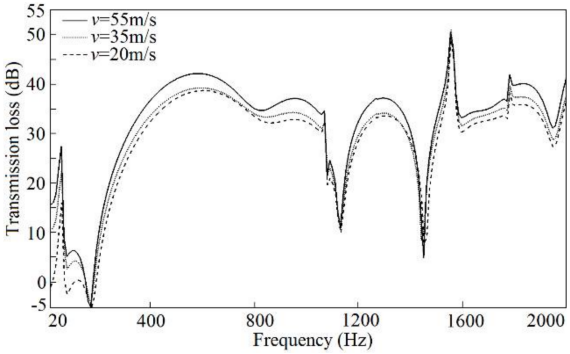

Figure 17. Effects of flow velocity on the *TL* of the silencer (T = 760 K).

5. Conclusions

This paper proposes a new approach—based on CFD results—to investigating the effects of temperature and flow velocity on the acoustic attenuation performance of a perforated tube silencer of a car. The validation results suggest that the proposed approach can make accurate predictions. In actual fact, the proposed approach is distinguished from the existing approaches by defining the fluid properties of every acoustic mesh element under the CFD results (including temperature and flow velocity). In doing so, the simplification of the temperature and flow velocity distribution is avoided, thus the effect can be predicted in greater detail. The results indicate that air flow velocity and temperature variation may have an effect on the investigated three-pass perforated tube silencer. An increase in temperature will shift the TL curve to a higher frequency and reduce the acoustic attenuation at most frequencies. As flow velocity increases and the curve is moved to a slightly lower frequency, the acoustic attenuation is enhanced, although the tendency is not particularly obvious. Additionally, the pressure loss of the perforated tube silencer can be calculated through the total pressure distribution from the CFD results. When the engine runs at 5500 r/min, the calculated value is approximately 37,710 Pa.

Acknowledgments: This work was supported by the National Natural Science Foundation of China (51275082, 11272273).

Author Contributions: Li-Xin Guo conceived and designed the research idea and the framework; Wei Fan performed the simulations; Hao Zhang analyzed the data and wrote the paper.

Conflicts of Interest: The authors declare no conflict of interest.

References

1. Shrivastava, A.K.; Tewari, V.K.; Santosh, K. Effect of Exhaust Back Pressure on Noise Characteristic of Tractor Mufflers. *AMA Agric. Mech. Asia* **2014**, *45*, 79–83.
2. Panigrahi, S.N.; Munjal, M.L. Backpressure Considerations in Designing of Cross Flow Perforated-element Reactive Silencers. *Noise Control Eng. J.* **2007**, *55*, 504–515. [CrossRef]
3. Bouldin, B.; Vunnam, K.; Hernanz-Manrique, J.A.; Ambit-Marin, L. CFD Analysis and Full Scale Testing of a Complex Auxiliary Power Unit Intake System. In Proceedings of the ASME Turbo Exposition, Vancouver, BC, Canada, 6–10 June 2011.
4. Chen, W.X.; Chong, D.T.; Yan, J.J.; Dong, S.C.; Liu, J.P. Numerical Investigation of Two-Phase Flow in Natural Gas Ejector. *Heat Transf. Eng.* **2014**, *35*, 738–745. [CrossRef]
5. Middelberg, J.M.; Barber, T.J.; Byme, K.P.; Leong, S.S.; Leonadi, E. *CFD Analysis of the Acoustic and Mean Flow Performance of Simple Expansion Chamber Mufflers*; ASME Paper No. IMECE2004-61371; ASME: New York, NY, USA, 2004.
6. Lee, S.H.; Ih, J.G. Effect of Non-Uniform Perforation in the Long Concentric Resonator on Transmission Loss and Back Pressure. *J. Sound Vib.* **2008**, *311*, 280–296. [CrossRef]
7. Ren, J.W.; Jiang, Q.Y.; Wang, Z. CFD Simulation and Computation of Pressure Loss of Resistance Muffler. In Proceedings of the 4th International Conference on Manufacturing Science and Engineering, Dalian, China, 30–31 March 2013.
8. Wylen, G.J.V.; Sonntag, R.E.; Borgnakke, C. *Fundamentals of Classical Thermodynamics*; Wiley: New York, NY, USA, 1985.
9. Wang, C.N.; Tse, C.C.; Chen, S.C. Flow Induced Aerodynamic Noise Analysis of Perforated Tube Mufflers. *J. Mech.* **2013**, *29*, 224–231. [CrossRef]
10. Sullivan, J.W. A Method for Modeling Perforated Tube Muffler Components: I. Theory; II. Applications. *J. Acoust. Soc. Am.* **1979**, *66*, 772–788. [CrossRef]
11. Sujith, R.I. Transfer Matrix of a Uniform Duct with an Axial Mean Temperature Gradient. *J. Acoust. Soc. Am.* **1996**, *100*, 2540–2542. [CrossRef]
12. Selamet, A.; Ji, Z.L. Acoustic Attenuation Performance of Circular Chambers with Single-inlet and double-outlet. *J. Sound Vib.* **2000**, *299*, 3–19. [CrossRef]

13. Kim, Y.H.; Choi, J.W.; Lim, B.D. Acoustic characteristics of an expansion chamber with constant mass flow and steady temperature gradient (theory and numerical simulation). *ASME J. Vib. Acoust.* **1990**, *112*, 460–467. [CrossRef]
14. Tsugi, T.; Tsuchiya, T.; Kagawa, Y. Finite Element and Boundary Element Modeling for the Acoustic Wave Transmission in Mean Flow Medium. *J. Sound Vib.* **2002**, *255*, 849–866. [CrossRef]
15. Kirby, R. A Comparison between Analytic and Numerical Methods for Modelling Automotive Dissipative Silencers with Mean Flow. *J. Sound Vib.* **2009**, *325*, 565–582. [CrossRef]
16. Broath, A.; Margot, X.; Gila, A. A CFD Approach to the Computation of the Acoustic Response of Exhaust Mufflers. *J. Comput. Acoust.* **2005**, *13*, 301–316. [CrossRef]
17. Sanchez-Orgaz, E.M.; Denia, F.D.; Martinez-Casas, J.; Baeza, L. 3D Acoustic Modelling of Dissipative Silencers with Nonhomogeneous Properties and Mean Flow. *Adv. Mech. Eng.* **2014**, *6*, 537935. [CrossRef]
18. Dong, H.L.; Deng, Z.X.; Lai, F. Analysis and Improvement of Muffler Acoustic Performance Considering Temperature Influence. *J. Vib. Eng.* **2009**, *22*, 70–75.
19. LMS Virtual. Lab. *LMS Virtual. Lab Online Help*; LMS International N.V.: Leuven, Belgium, 2013; Volume 11.
20. Guo, L.X.; Fan, W. A comparison between various numerical simulation methods for predicting the transmission loss in silencers. *J. Eng. Res.* **2017**, *5*, 163–180.
21. Lee, S.H.; Ih, J.G. Empirical Model of the Acoustic Impedance of a Circular Orifice in Grazing Mean Flow. *J. Acoust. Soc. Am.* **2003**, *114*, 98–113. [CrossRef] [PubMed]
22. Liu, C.; Ji, Z.L. Computational Fluid Dynamics-Based Numerical Analysis of Acoustic Attenuation and Flow Resistance Characteristics of Perforated Tube Silencers. *ASME J. Vib. Acoust.* **2014**, *136*, 21006. [CrossRef]
23. *ANSYS Fluent 12.1 in Workbench User's Guide*; ANSYS Worbench 12.1; ANSYS Inc.: New York, NY, USA, 2009.
24. Fang, J.H.; Zhou, Y.Q.; Hu, X.D.; Lin, Z.S. Study on Aerodynamic Quality and Fluid Simulation of Expansion Mufflers. *J. Syst. Simul.* **2009**, *21*, 6399–6404.
25. Pan, D.Y.; Sun, J.Q.; Fang, D.Q.; Dong, J.Y. Research and Application on Flow Characteristics of Muffler. *Noise Vib. Control* **1984**, *5*, 9–14.
26. Karlsson, M.; Abomb, M. Aeroacoustics of T-Junctions—An Experimental Investigation. *J. Sound Vib.* **2010**, *329*, 1793–1808. [CrossRef]
27. Zhan, F.L.; Xu, J.W. *Virtual. Lab Acoustics Simulation from Entry to Master*; Northwestern Polytechnical University Press: Xi'an, China, 2013.